Modeling Buckminsterfullerene Spinning in (C 60) n Clusters

ARTICLE *in* JOURNAL OF THE AMERICAN CHEMICAL SOCIETY · JUNE 1999

Impact Factor: 12.11 · DOI: 10.1021/ja980846r

2 AUTHORS, INCLUDING:

Michael S Deleuze
Hasselt University
132 PUBLICATIONS **2,672** CITATIONS

Modeling Buckminsterfullerene Spinning in $(C_{60})_n$ Clusters

Michael S. Deleuze[†] and Francesco Zerbetto*[,‡]

Contribution from Departement SBG, Limburgs Universitair Centrum, Universitaire Campus, B3590 Diepenbeek, Belgium, and Dipartimento di Chimica "G. Ciamician", Università degli Studi di Bologna, Via F. Selmi 2, 40126 Bologna, Italy

Received March 16, 1998. Revised Manuscript Received March 29, 1999

Abstract: Temperature-dependent rate constants for the spinning of buckminsterfullerene in $(C_{60})_n$ clusters ($n = 3-13$) are calculated using unimolecular reaction rate theory with parameters obtained from molecular mechanics simulations. The lowest lying intracluster rotations tend to spread over several cages toward the surface and the edges of the clusters. Coaxial rotations appear also in this regime. A simple argument is put forward to justify the use of harmonic spacing in the study of the dynamics of these degrees of freedom. The increase in the size of the cluster makes the calculated rate constants converge toward the value reported in the solid. The satisfactory result of this simple form of kinetic theory implies that the energy of the internal degrees of freedom is randomized sufficiently fast with respect to the spinning coordinates.

1. Introduction

Buckminsterfullerene is probably one of the most significant success stories in the investigation of the appearance of magic numbers in the size of clusters.[1] Its many interesting properties stem from a fully conjugated π-electron system wrapped around a nearly spherical surface. Sphericity allows C_{60} to spin in the solid and in benzene-like solvates[2] and is also responsible for the existence of $(C_{60})_n$ clusters resembling those formed by giant rare-gas atoms.[3] While nearly-free rotation is likely to be also present in the positively charged $(C_{60})_n$ clusters produced in mass spectroscopic experiments,[3] their charge and their relatively low temperature—which was evaluated to be roughly 130 K[3]—probably make the corresponding rate constants too low to measure experimentally. In the solid, instead, the room-temperature rate of rotation of C_{60} was found to be higher than 10^9 s^{-1}. In particular, the 10^9 s^{-1} value is already reached at 233 K while it is essentially frozen below 123 K.[2b] A value of 1.8×10^{10} s^{-1} was also reported at 283 K.[2a] From a chemical point of view, the study of the dynamics of buckminsterfullerene appears to be of particular interest since the reorientational times of C_{60} were found not to conform to conventional viscosity arguments and hydrodynamic-based models proved to be unsuccessful in their simulation.[2f] A successful treatment would therefore afford a deeper insight into the properties of bulk C_{60}.

To date the computational investigation of $(C_{60})_n$ clusters has used a number of potentials.[4] A very large number of stationary points was located. However, while their structures are now known, much of their dynamics remains to be investigated both experimentally and theoretically. The rotation of C_{60} cages in large Van Der Vaals clusters and in the solid phase is a challenging question, as this motion is driven by the balance between weak intermolecular forces and the energy flow between many internal degrees of freedom accounting for inter- and intramolecular vibrations. Identification of models able to simulate it can thus be instrumental to further our understanding of the many complicated phenomena which grace the chemistry and physics of C_{60}.

The simplest kinetic models are based on unimolecular reaction rate theory and require activation energies and vibrational frequencies as input parameters[5] which, in this case, can be calculated with molecular mechanics programs. Merits and shortcomings of several types of these approaches have been re-examined recently.[6−10] In the past, unimolecular reaction rate

[†] Limburgs Universitair Centrum.

[‡] Università degli Studi di Bologna.

(1) (a) Kroto, H. W.; Heath, J. R.; O'Brien, S. C.; Curl, R. F.; Smalley, R. E. *Nature* **1985**, *368*, 6042. (b) Krätschmer, W.; Lamb., L. D.; Fostiropoulos, K.; Huffman, D. R. *Nature* **1990**, *347*, 354.

(2) (a) Johnson, R. D.; Yannoni, C. S.; Dorn, H. C.; Salem, J. R.; Bethune, D. S. *Science* **1992**, *255*, 1235. (b) Tycko, R.; Haddon, R. C.; Dabbagh, G.; Glarum, S. H.; Douglass, D. C.; Mujsce, A. M. *J. Phys. Chem.* **1991**, *95*, 518. (c) Yannoni, C. S.; Johnson, R. D.; Mejer, G.; Bethune, D. S.; Salem, J. R.; *J. Phys. Chem.* **1991**, *95*, 9. (d) Fischer, J. E.; Heiney, P. A.; Smith, A. B., III. *Acc. Chem. Res.* **1992**, *25*, 112. (e) He, H.; Barras, J.; Foulkes, J.; Klinowski, J., *J. Phys. Chem. B* **1997**, *101*, 117. (f) Shang, X.; Issa, M. H.; Rodriguez, A. A. *J. Phys. Chem. A* **1998**, *102*, 7731.

(3) (a) Martin, T. P.; Näher, U.; Schaber, H.; Zimmermann, U. *Phys. Rev. Lett.* **1993**, *70*, 3079. (b) Winter, B.; Mitzner, R.; Kusch, Ch; Campbell, E. E. B.; Hertel, I. V. *J. Chem. Phys.* **1996**, *104*, 9179. (c) Hansen, Hohmann, H.; Müller, R.; Campbell E. E. B. *J. Chem. Phys.* **1996**, *105*, 6088.

(4) (a) Wales, D. J. *J. Chem. Soc., Faraday Trans.* **1994**, *90*, 1061. (b) Wales, D. J. *J. Chem. Phys.* **1994**, *101*, 3750. (c) Doye, J. P. K.; Wales, D. J.; *Chem. Phys. Lett.* **1995**, *247*, 339. (d) Doye, J. P. K.; Wales, J. D. *Chem. Phys. Lett.* **1996**, *262*, 167. (e) Doye, J. P. K.; Dullweber, A.; Wales, D. J. *Chem. Phys. Lett.* **1997**, *269*, 408.

(5) See e.g.: (a) Gilbert, R. C.; Smith, S. C. *Theory of Unimolecular and Recombination Reactions*; Blackwell Scientific Publications: Oxford, U.K., 1990. (b) Pilling, M. J.; Seakins, P. W. *Reaction Kinetics*; Oxford University Press: Oxford, U.K., 1995. (c) Baer. T.; Hase, W. L. *Unimolecular Reaction Dynamics, Theory and Experiment*; Oxford University Press: Oxford, U.K., 1996. (d) Steinfeld, J. I.; Francisco, J. S.; Hase, W. L. *Chemical Kinetics and Dynamics*, 2nd ed.; Prenctice Hall, Engineering, Science and Math.: New Jersey, 1998.

(6) Truhlar, D. G.; Garrett, B. C.; Klippenstein, S. J. *J. Phys. Chem.* **1996**, *100*, 12771 and references therein.

(7) (a) Khundkar, L. R.; Marcus, R. A.; Zewail, A. H. *J. Phys. Chem.* **1983**, *87*, 2473. (b) Troe, J. *Chem. Phys. Lett.* **1985**, *114*, 241. (c) Felker, P. M.; Zewail, A. H. *J. Phys. Chem.* **1985**, *89*, 5402. (d) Negri, F.; Orlandi, G. *J. Phys. Chem.* **1991**, *95*, 748.

(8) (a) Syage, J. A.; Lambert, W. R.; Felker, P. M.; Zewail, A. H.; Hochstrasser, R. M. *Chem. Phys. Lett.* **1982**, *88*, 266. (b) Amirav, A.; Jortner, J. *Chem. Phys. Lett.* **1983**, *95*, 295. (c) Majors, T. J.; Even, U.; Jortner, J. *J. Chem. Phys.* **1984**, *81*, 2330. d) Syage, J. A.; Felker, P. M.; Zewail, A. H. *J. Chem. Phys.* **1984**, *81*, 4706.

(9) (a) Wang, H. B.; Goldfiled, E. M.; Hase, W. L.; *J. Chem. Soc., Faraday Trans.* **1997**, *93*, 737. (b) Wang, H. B.; Hase, W. L. *J. Am. Chem. Soc.* **1997**, *119*, 3093. (c) Peslherbe, G. H.; Wang, H. B.; Hase, W. L. *J. Am. Chem. Soc.* **1996**, *118*, 2257.

(10) Miller, W. H. *J. Phys. Chem. A* **1996**, *102*, 793.

10.1021/ja980846r CCC: $18.00
Published on Web 05/25/1999

theory (e.g., Rice, Ramsperger, Kassel, and Marcus (RRKM)) has found application in many cases.[5] An example, which is rather similar in terms of the rate constants and activation barriers to the present case, is the electronically excited-state isomerization of stilbene[7,8] which was simulated also by a combination of molecular modeling and RRKM theory.[7] The energy barrier for stilbene is slightly less than 4 kcal/mol with rate constants in the nanosecond regime (see below for C_{60}).

In this paper, we discuss the temperature-dependent (Boltzmann-averaged) intermolecular dynamics of C_{60} clusters. A simple argument is put forward to show that, although the associated potentials must be anharmonic, most of these vibrations must possess harmonic spacing. The calculations of the rate constants for the intercage motions are shown to converge toward the solid-state value.

2. Theoretical and Methodological Background

2a. Calculation of Kinetic Rate Constants. Microscopic rate constants are evaluated in the context of unimolecular reactions, using RRKM theory[5] as

$$k(E) = \frac{\int_0^{E-E_0} \rho^{\ddagger}(E - E_0 - E_s)\, dE_s}{h\, \rho(E)} \qquad (1)$$

This expression is derived from an evaluation of flux trajectories in phase space, under the assumption of ergodicity and through consideration of a microcanonical ensemble of reactant states at a given energy E. In the equation, E_0 represents the critical (activation) energy of the transition state, E_s is the excess (kinetic) energy at the saddle point, and ρ and $\rho^{\ddagger}$ are the density of states of the reference (ground state) reactant structure and of the transition state, respectively. Since the results of the calculations are compared with data obtained in the solid phase, macroscopic (i.e., temperature-dependent) rate constants are obtained in the high-pressure limit, via Boltzmann averaging, as

$$k(T) = \frac{\int_{E_0}^{\infty} dE\, k(E)\, \rho(E)\, e^{-E/k_B T}}{\int_0^{\infty} dE\, \rho(E)\, e^{-E/k_B T}} = \frac{k_B T}{h} \frac{Q^{\ddagger}}{Q} e^{-E_0/k_B T} \qquad (2)$$

an approach which is most commonly referred to as transition-state theory[5] (TST). In the actual calculations reported in this work, eq 2 uses the vibrational partition functions of the minimum, Q, and of the transition state, $Q^{\ddagger}$. These are obtained in the harmonic approximation, using

$$Q = \prod_i (1 - e^{-\hbar\omega_i/k^B T})^{-1} \qquad (3)$$

Ergodicity is essential in deriving and applying eq 1. This assumption is equivalent to the requirement of rapid energy randomization throughout the vibrational normal modes on the time scale of the transition. Since our aim is to investigate motions on the nanosecond time scale, it should be noted that this assumption may partially break down because of the very low vibrational frequencies, down to 3 cm^{-1} or ~90 GHz, encountered in C_{60} clusters (see below). TST calculations of temperature-dependent rate constants are thus also of interest to evaluate whether the assumption of random energy transfers is valid or not in this case. It is believed, in practice, that the exploration of the configurational space can be regarded as mostly complete on this time scale, considering the numerous degrees of freedom present in these clusters.

The harmonic approximation may also be a drastic simplification for intermolecular modes with frequencies as low as a few cm^{-1}. However, the large mass of the rotating cages drives their vibrational spacing toward harmonicity (for an example, see below).

2b. The Force Field. To avoid bias in the selection of parameters employed in the unimolecular reaction rate theories,[5] TST rate constants were calculated using the general MM3 molecular mechanics force field.[11,12] The advantage of the use of this traditional model over procedures developed ad hoc for fullerenes is the ample parametrization which may enable future extensions to related guest−host systems such as, for instance, the well-known adducts that C_{60} forms with calixarenes.[13] The most demanding part of MM3 model[11,12] is the π-electron SCF evaluation of the stretching and torsional parameters of the conjugated bonds. Such calculations become quickly untractable for large C_{60} clusters. To overcome this difficulty and apply consistently this force field to systems as large as $(C_{60})_{13}$, we used the MM3 force constants obtained for a single C_{60} unit, i.e., we considered that the cohesion forces in the cluster do not significantly affect the π-electron density. This fact was independently verified for the smaller clusters.

3. Results and Discussion

3a. The Intermolecular Vibrations. The minima of the MM3 model correspond closely to those obtained with other methods,[4] and it is deemed not necessary to discuss them here**.** Among the $6n - 6$ low-wavenumber intercage vibrations of a $(C_{60})_n$ cluster, inspection shows that the first $3n$ modes, typically in the 2−14 cm^{-1} range, can be described as (hindered) rotations, while at higher frequencies (14−60 cm^{-1}), the remaining, $3n - 6$, vibrations correspond to distortions of the cluster structure (i.e., collective deformations of the sphere packing). Only minor differences were noticed between the modes of minima and transition states. The distribution of the intercage modes for the largest cluster, namely $(C_{60})_{13}$, is shown in Figure 1. All of these intermolecular vibrational modes fall at much lower energy than the intramolecular vibrations[14] and dominate the RRKM/TST expressions of the kinetic rate constants. In particular, using[15] the Beyer−Swineheart algorithm,[16] we found that the density of states calculated using only the wavenumbers of the intermolecular vibrations is practically identical to that obtained with the full set of modes.

(11) (a) Allinger, N. L.; Yuh, Y. H.; Lii, J.-H. *J. Am. Chem. Soc.* **1989**, *23*, 8551. (b) Lii, J.-H.; Allinger, N. L. *J. Am. Chem. Soc.* **1989**, *23*, 8566. (c) Lii, J.-H.; Allinger, N. L. *J. Am. Chem. Soc.* **1989**, *23*, 8576.

(12) The MM3 calculations were run with the Tinker program: (a) Ponder, J.; Richards, F. *J. Comput. Chem.***1987**, *8*, 1016. (b) Kundrot, C.; Ponder, J.; Richards, F. *J. Comput. Chem.* **1991**, *12*, 402−409. (c) Dudek, M. J. Ponder, *J. Comput. Chem.* **1995**, *16*, 791.

(13) (a) Atwood, J. L.; Koutsantonis, G. A.; Raston, C. L. *Nature* **1994**, *368*, 229. (b) Suzuki, T.; Nakashima, K.; Shinkai, S. *Chem. Lett.* **1994**, 699. (c) Araki, K.; Kiyotaka, A.; Ikeda, A.; Suzuki, T.; Shinkai, S. *Tetrahedron Lett.* **1996**, *37*, 73. (d) Haino, T.; Yanase, M.; Fukazawa, Y. *Angew. Chem., Int. Ed. Engl.* **1997**, *36*, 259. (e) Atwood, J. L.; Barbour, L. J.; Raston, C. L.; Sudria, I. B. N. *Angew. Chem., Int. Ed. Engl.* **1998**, *37*, 981. (f) Haino, T.; Yanase, M.; Fukazawa, Y. *Angew. Chem., Int. Ed. Engl.* **1998**, *37*, 997.

(14) For a review, see: Kuzmany, H.; Matus. M.; Burger, B.; Winter, J. *Adv. Mater.* **1994**, *6*, 731.

(15) The rate constant and densities of states were calculated using: Gilbert, R. G.; Jordan, M. J. T.; Smith, S. C. UNIMOL program suite (Calculation of falloff curves for unimolecular and recombination reactions), 1993.

(16) (a) Beyert, T.; Swinehart, D. *Commun. Assoc. Comput. Machines* **1973**, *16*, 379. (b) Stein, S.; Rabinovitch, B. *J. Chem. Phys.* **1973**, *58*, 2438−2445.

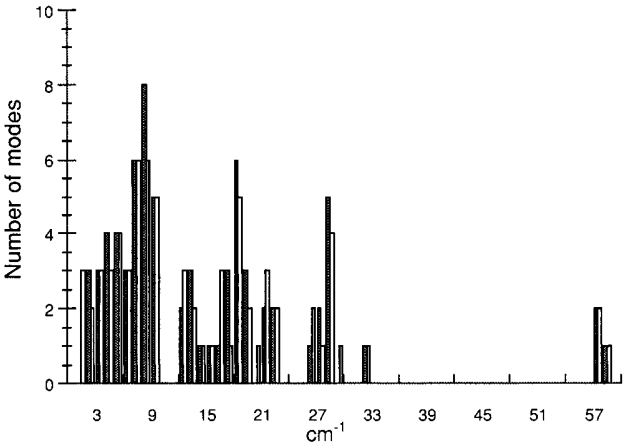

Figure 1. Distribution of intermolecular modes for $(C_{60})_{13}$. Both the reactant (black) and the transition-state (white) modes are shown.

Table 1. Energies (cm^{-1}) of the First 27 Vibrational Levels for the Hindered Rotor $-B(d^2/d\varphi^2) + (1/2)V_3(1 - \cos 3\varphi)$ (where $B = 0.01$ cm^{-1} and $V_3 = 500$ cm^{-1})[a]

n	*E*	*n*	*E*	*n*	*E*	*n*	*E*	*n*	*E*
0	4.74	1	14.20	2	23.64	3	33.06	4	42.46
5	51.83	6	61.18	7	70.51	8	79.81	9	89.09
10	98.35	11	107.59	12	116.80	13	125.98	14	135.15
15	144.29	16	153.40	17	162.50	18	171.56	19	180.61
20	189.63	21	198.62	22	207.59	23	216.54	24	225.46
25	234.36	26	243.23	27	252.07				

[a] Despite the anharmonic nature of the potential, the spacing is harmonic.

A point worth investigating is the validity of the harmonic approximation in the calculation of the density of states due to the intercage modes. In principle, the Beyer−Swineheart algorithm can be used and upgraded to include anharmonic spacing.[16] In practice, however, serious difficulties with the evaluation of rate constants are then to be expected from a necessary[15] numerical integration over exceedingly huge densities of states. Previous experience with torsional potentials,[17] furthermore made us believe that, because of the large masses involved in these vibrations, such a treatment is not necessary. As an example, one can consider the energy levels of a hindered rotor of 3-fold symmetry; higher or lower symmetries would not change the argument. The rotor consists of (at least) two C_{60}s rotating out-of-phase about an axis. The corresponding model Hamiltonian reads

$$H = -B\frac{d^2}{d\varphi^2} + \frac{1}{2}V_3(1 - \cos 3\varphi) \qquad (4)$$

where B is the reduced B, as in the case of a reduced mass, of isolated C_{60} which can be estimated using C_{60} bond lengths as $\sim$0.03 cm^{-1}. If one sets B in eq 4 to 0.01 cm^{-1} and the energy barrier $V_3 = 500$ cm^{-1}, that is less than 1.5 kcal/mol, the first 27 energy levels are given in Table 1. They show harmonic spacing all the way up to the onset of intramolecular vibrations. Participation of more cages would result in a larger B, which, in turn, would make the spacing even more harmonic.

3b. The Transition States. The transition states listed in Table 2 were located relaxing the system to the closest transition state after partial rotation of one of the C_{60}s. For the larger clusters, $n = 8-13$, rotation was imposed only to the cage with the maximum number of direct neighbors. The lowest lying transition states found for the present set of clusters are displayed in Figure 2. Each C_{60} is depicted as a connectivity center together with the vector of its rotational moment. The moments provide a simple representation of the motions at the transition state, since they give both the orientation of the rotational axis and the weight of each C_{60} in the motion. From the figure, rotations obviously tend to delocalize to several spheres and propagate to the surface and edges of the clusters, to limit frictions with direct neigbors. This figure also shows that the spreading of rotations among the cages is mostly limited to the nearest neighbors of the rotating C_{60}.

Table 2. Characterization of the Transition States and Corresponding Room Temperature TST Rate Constants for the Rotation of Buckmisterfullerene in $(C_{60})_n$ Clusters[a]

n	$\Delta H^{\dagger}$ (kcal/mol)	$\tilde{\nu}$ (i cm^{-1})	$\langle N_d \rangle$	k (s^{-1})	k' (s^{-1})
3	0.17	3.27	2.00	3.22×10^{10}	3.22×10^{10}
	0.24	4.38	2.00	5.07×10^{10}	5.08×10^{10}
	0.32	5.89	2.00	5.96×10^{10}	5.88×10^{10}
4	0.27	5.42	3.00	3.30×10^{11}	3.32×10^{11}
	0.32	3.68	3.00	1.19×10^{11}	1.19×10^{11}
5	0.19	3.26	3.36	4.17×10^{10}	4.15×10^{10}
	0.29	3.72	3.88	8.98×10^{10}	8.94×10^{10}
	0.28	3.33	3.79	4.33×10^{11}	4.45×10^{11}
	0.37	4.29	3.82	8.10×10^{10}	8.11×10^{10}
	0.29	4.38	3.56	1.73×10^{11}	1.73×10^{11}
	0.46	2.82	3.80	5.32×10^{10}	5.33×10^{10}
	0.48	3.87	3.16	8.99×10^{10}	8.96×10^{10}
	0.58	4.38	3.19	1.38×10^{11}	1.37×10^{11}
	1.09	5.43	3.10	8.66×10^{10}	8.64×10^{10}
6	0.28	4.25	4.00	4.81×10^{11}	4.82×10^{11}
	0.29	4.59	4.00	7.53×10^{11}	7.51×10^{11}
	0.37	5.86	4.00	3.55×10^{11}	3.56×10^{11}
	0.46	5.21	4.00	9.91×10^{10}	9.95×10^{10}
7	0.75	3.34	4.11	9.11×10^{10}	9.09×10^{10}
	0.83	4.01	4.80	1.61×10^{11}	1.61×10^{11}
	1.09	3.31	4.64	9.27×10^{10}	9.20×10^{10}
8	0.64	3.37	5.65	2.64×10^{11}	2.64×10^{11}
	0.81	6.52	4.31	5.14×10^{11}	5.12×10^{11}
	1.16	3.11	5.91	1.05×10^{12}	1.05×10^{12}
9	0.54	4.04	6.10	1.14×10^{12}	1.15×10^{12}
	1.03	2.21	5.09	2.72×10^{11}	2.74×10^{11}
10	0.61	4.07	4.77	8.91×10^{10}	8.95×10^{10}
11	0.22	2.74	5.28	5.81×10^{10}	5.85×10^{10}
	1.15	6.24	8.19	3.61×10^{9}	3.63×10^{9}
12	1.72	5.37	8.67	4.41×10^{10}	4.42×10^{10}
13	2.04	3.45	7.03	8.91×10^{10}	8.92×10^{10}

[a] Considering all vibrational modes (k) or the intermolecular vibrational modes only (k') (see text).

In Table 2, the MM3 activation energies, $\Delta H^{\dagger}$, include zero-point energies. The imaginary wavenumbers corresponding to the negative curvature at the top of the transition state, $\tilde{\nu}$, are given along with the average number of direct neighbors involved in the rotations.[18] The normal modes with negative curvature—which characterize the transition states—have values of wavenumbers up to 7i cm^{-1}. Similar values, up to 5i cm^{-1}, were found before in the investigation of $(C_{60})_n$ clusters with the Lennard-Jones potential.[4] To understand this nearly constant value, one ought to consider that the reduced mass increases with the size of the cluster because the rotation of a fullerene tends to be accompanied by the movement, in the opposite direction, of the other molecules in the cluster (see Figure 3).

(17) (a) Siebrand, W.; Zerbetto, F.; Zgierski, M. Z. *J. Chem. Phys.* **1989**, *91*, 5926. (b) Siebrand, W.; Zerbetto, F.; Zgierski, M. Z. *Chem. Phys. Lett.* **1990**, *174*, 119.

(18) The number of C_{60} neighboring molecules, $\langle N_d \rangle$, involved in the rotation at the transition state is defined as a sum over all the C_{60}s of their individual contributions, $\langle N_d \rangle = \sum_J W_J F_J$, in which F_J represents the conventional number of direct neighbors in the packing [e.g., 12 for the central C_{60} in $(C_{60})_{13}$]. The weight factors are obtained as $W_J = \sum_{i \in J} ||L_i||^2$, with L_i being the atomic displacements associated to the imaginary curvature at the top of the barrier. Within the solid phase, $\langle N_d \rangle$ should be equal to 12.

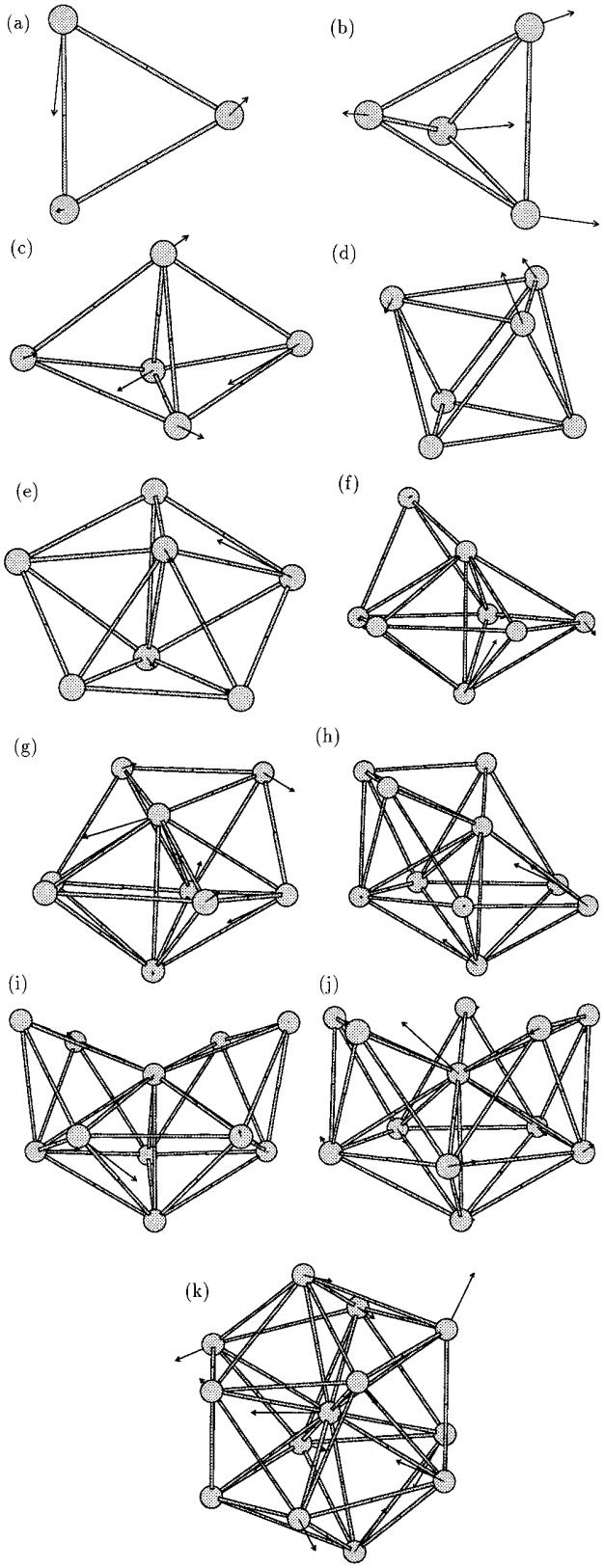

Figure 2. Pictorial representation of the lower transition states found for the clusters considered in this study. Rotations are represented by the rotational moments of the individual fullerenes, $\vec{R}_J = \sum_{i \in J} m_i \vec{L}_i \times (\vec{r}_i - \vec{r}_{iJ})$, with $\vec{r}_i$ and $\vec{r}_{iJ}$ being the coordinates of carbon atoms and of their projection on the rotation axis of sphere *J*. A threshold of 9.2 Å on the interdistances between centers of cages has been considered to establish connectivities.

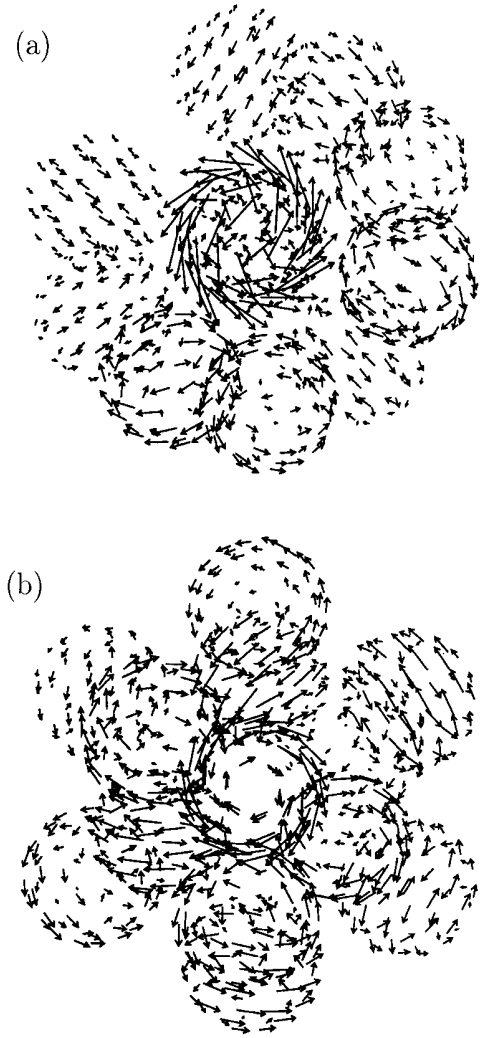

Figure 3. The transition states for the rotation of the central C_{60} in (a) $(C_{60})_{12}$ and (b) $(C_{60})_{13}$. The arrows display the normal mode with negative curvature for the transition state of the spinning of the central fullerene. The fullerenes are not show to help the eye to perceive the rotations.

The effect of the masses is counteracted by an increase of the force due to the increased barrier.

In general, lower values of the energy barriers—and larger rate constants, see below—correspond to the rotations of fullerenes only partially surrounded by other molecules in the cluster (also see the $\langle N_d \rangle$ values[18] of Table 2). Coaxial rotations appear to be favored since, in many cases, rotational moments are roughly aligned. Inspection of Table 2 and Figure 4 shows that the activation barrier tends to increase with the number of fullerenes in the cluster. For values of *n* close to the "magic" number 13, for which the central sphere is perfectly shrouded by the other spheres, and despite the delocalization of rotations, it is already ~2 kcal/mol. As expected, the larger the number of surrounding C_{60}s the higher the barrier. Extrapolation of these data to a full coverage ($\langle N_d \rangle = 12$) gives an estimate for the rotational barriers ranging from 2.2 to 3.0 kcal/mol, according to a linear and a quadratic fit, respectively. These values belong to the range of the two apparent activation energies reported[2] in the solid: 1.4 ± 0.1 kcal/mol and 4.2 ± 1.2 kcal/mol, for a (nearly free) *rotator* phase at high temperature ($T > 260$ K) and the so-called *ratchet* phase, characterized by jump rotational diffusions at low temperatures, respectively.

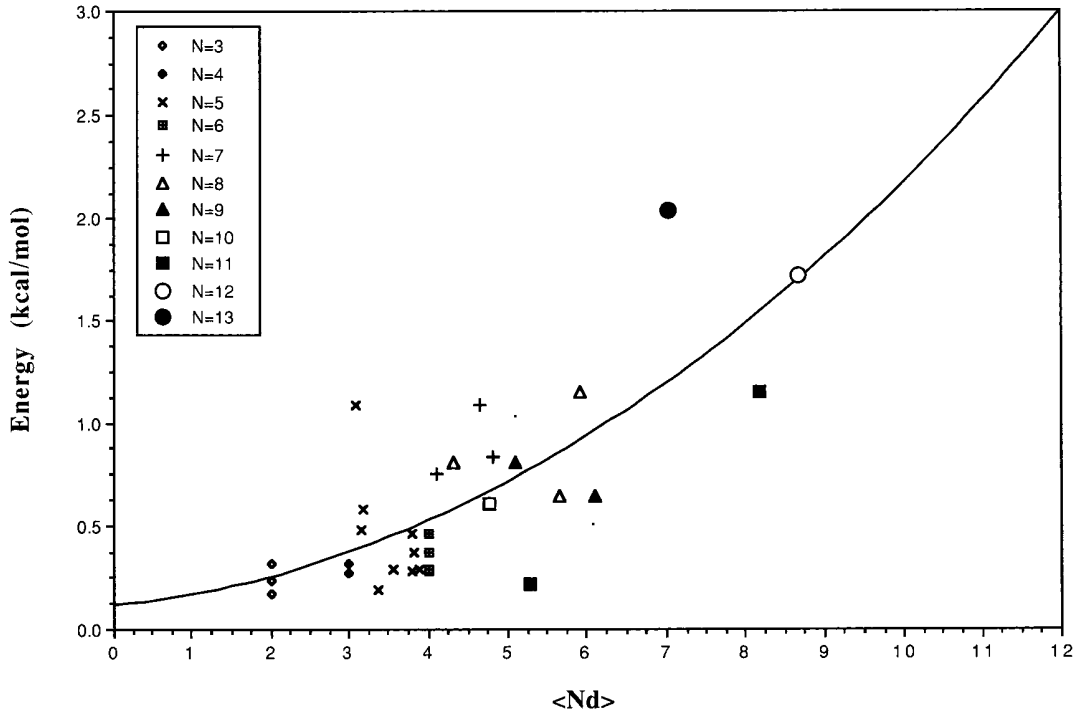

Figure 4. Activation energies for the motions in $(C_{60})_n$, $n = 3-13$, clusters as a function of the N_d coverage.

Of particular interest, possibly even for a comparison with the solid-phase data, are the transition states identified for $(C_{60})_{12}$ and $(C_{60})_{13}$. From the geometric point of view (Figure 3, but see also Figure 2j,k and the $\langle N_d \rangle$ values of Table 2), these structures resemble what may be found close to the surface or in the bulk. Inspection shows that the number of cages involved in the rotation is lower, and the barrier is correspondingly smaller, when the cage rotates about a (nearly) 5-fold axis (Figure 3a) rather than a (nearly) 3-fold one (Figure 3b). This is due to the fact that rotation about the former axis generates more equatorial frictions.

3c. The Rate Constants. The room-temperature rate constants (k)[19] shown in Table 2 were evaluated using the complete set of calculated vibrations. The last column of the table, k'_{TST}, shows the kinetic rate constants obtained by restricting the calculations to the $6n - 6$ intermolecular low-frequency vibrational modes. As can be seen, the removal of the high-frequency intramolecular modes has little effect on the results obtained using TST. This is expected since the partition functions for the intramolecular modes are nearly identical for the molecule and the transition state.

According to TST, the calculated room-temperature rate constants are on average between 10^{10} and 10^{11} s^{-1}. In an experiment, slower motions would be washed out by the faster ones. For the largest clusters, the calculated room-temperature rate constants slightly exceed the experimental ones for the bulk. For the ideally localized rotation ($\langle N_d = 8.7 \rangle$) of the cage at the center of $(C_{60})_{12}$, TST obtains at 298 and 283 K rate constants of 4.41×10^{10} and 3.77×10^{10} s^{-1}, respectively. These values appear to have the correct order of magnitude, in view of the likely higher viscosity of the solid and of the experimental rate constants higher than 10^9 s^{-1} obtained for cage spinning, at room temperature (in particular with the value of 1.8×10^{10} s^{-1} reported at 283 K[2a]).

(19) In the event that experiments were to become available at any other temperature, the authors would gladly provide the relevant constants (see, however, Table 3).

Table 3. Temperature Dependence of the TST Rate Constants for the Rotational Transition State Identified for the $(C_{60})_{12}$ and $(C_{60})_{13}$ Clusters for Different Activation Energies[a]

	$(C_{60})_{12}$		
T (K)	k (s^{-1}) ($E = 1.72$ kcal/mol)	k^* (s^{-1}) ($E = 3.0$ kcal/mol)	k^* (s^{-1}) ($E = 4.2$ kcal/mol)
298	4.41×10^{10}	5.25×10^{9}	6.70×10^{8}
283	3.77×10^{10}	4.01×10^{9}	4.59×10^{8}
233	1.94×10^{10}	1.28×10^{9}	9.18×10^{7}
183	6.96×10^{9}	2.18×10^{8}	7.62×10^{6}
133	1.15×10^{9}	9.81×10^{6}	9.74×10^{4}
123	6.79×10^{8}	3.90×10^{6}	2.66×10^{4}
103	1.70×10^{8}	3.60×10^{5}	933
83	2.20×10^{7}	1.06×10^{4}	6.51
73	5.18×10^{6}	875	0.196
63	7.73×10^{5}	0.359	1.94×10^{-3}
53	5.53×10^{4}	4.78×10^{-4}	3.37×10^{-6}
	$(C_{60})_{13}$		
T (K)	k (s^{-1}) ($E = 2.04$ kcal/mol)	k^* (s^{-1}) ($E = 3.0$ kcal/mol)	k^* (s^{-1}) ($E = 4.2$ kcal/mol)
298	8.91×10^{10}	8.23×10^{9}	1.08×10^{9}
283	7.41×10^{10}	6.27×10^{9}	7.43×10^{8}
233	3.36×10^{10}	1.97×10^{9}	1.14×10^{8}
183	8.97×10^{9}	3.29×10^{8}	1.21×10^{7}
133	1.15×10^{9}	1.32×10^{7}	1.52×10^{5}
123	5.70×10^{8}	5.60×10^{6}	4.13×10^{4}
103	1.94×10^{8}	5.03×10^{5}	1430
83	9.52×10^{6}	1.41×10^{4}	9.78
73	1.70×10^{6}	1140	0.291
63	1.76×10^{4}	41.2	2.83×10^{-3}
53	8.31×10^{3}	0.427	4.81×10^{-6}

[a] The k^* values correspond to barriers higher than the MM3 calculated one.

From inspection of the results reported in Table 2, the TST approach appears overall to yield fairly stable and consistent rate constants, despite the rather "flat" nature of some of the transition states, some of which are characterized by very low imaginary wavenumbers ($\leq 3-3.2$ cm^{-1}) and vibrational frequencies (≤ 3 cm^{-1}). The absence of a rather net influence of

the activation energies onto the calculated rate constants indicate that the process of cage spinning is mostly governed by density-of-states and inertia effects. The rather satisfactory result of this simple form of kinetic theory suggests that the assumption of fast energy transfer on the time scale of the process (ergodicity) is valid.

In Table 3, the rate constants are shown for selected temperatures and the barrier obtained with the MM3 model plus two additional, higher, energy barriers, corresponding to the extrapolated value of 3.0 kcal/mol at a full coverage $\langle N_d \rangle = 12$ and the low-temperature experimental value of 4.2 kcal/mol[2]. The calculated data show that a barrier of 3.0 kcal/mol enables rotational frequencies faster than 10^9 s^{-1} above 233 K and a decrease of rate constants by more than 5 orders of magnitude when cooling to 100 K, a temperature at which the rotational correlation time in the bulk is reported to be greater than 50 μs.[2b]

Conclusions

In conclusion, temperature-dependent, i.e. Boltzmann-averaged, unimolecular reaction rate theory calculations show that the rate of rotations in $(C_{60})_n$ clusters, $n = 3-13$, converge toward the value reported for the solid phase. The room-temperature rate constants belong to the nanosecond regime, with activation energies ranging from 0.2 to 2.0 kcal/mol. Extrapolation to perfect coverage of C_{60} with 12 cages gives an activation energy that ranges from 2.2 to 3.0 kcal/mol.

As with any model, the success of the present approach does not necessarily imply that the theory offers the most realistic description of the dynamics. However, since the parameters were obtained from an independent set of calculations, it is believed that they can provide a first, reasonable step toward the description of C_{60} spinning in the solid and in organic matrices (cyclodextrines and calixarenes[13]). The dynamics in these complexes should, in principle, be simpler to describe because of the fewer molecules that are involved.

Acknowledgment. M.S.D. thanks the FWO_Vlaanderen, Flemish Fund for Scientific Research, for his position as a Senior Research Assistant of Prof. J.-P. François at the Limburgs Universitair Centrum. F.Z. gratefully acknowledges support from CNR through the program “Materiali Innovativi (legge 95/95)”.

JA980846R